Al-Azhar Bulletin of Science

Volume 17 | Issue 2 Article 7

12-1-2006
Section: Botany, Microbiology and Zoology

ELECTROCHEMICAL BEHAVIOR OF TITANIUM ELECTRODE IN AQUEOUS BROMIDE SOLUTIONS

ENAS ATTIA
Chemistry Department, Faculty of science (for girls), AL- Azhar University, Cairo, Egypt.

How to Cite This Article
ATTIA, ENAS (2006) "ELECTROCHEMICAL BEHAVIOR OF TITANIUM ELECTRODE IN AQUEOUS BROMIDE SOLUTIONS," *Al-Azhar Bulletin of Science*: Vol. 17: Iss. 2, Article 7.
DOI: https://doi.org/10.21608/absb.2006.11653

Al-Azhar Bull. Sci. Vol. 17, No. 2 (Dec.): pp. 53-71, 2006

ELECTROCHEMICAL BEHAVIOR OF TITANIUM ELECTRODE IN AQUEOUS BROMIDE SOLUTIONS

ENAS M. ATTIA

Chemistry Department, Faculty of science (for girls), AL- Azhar University, Cairo, Egypt.

Abstract

The behavior of Ti electrode in some bromide solutions of HBr, NaBr and $MgBr_2$ was studied using different techniques (open circuit potential, potentiostatic, potentiodynamic and galvanostatic polarization).

The obtained results revealed that in the three different bromide solutions there was a tendency of Ti for passivation. Titanium was susceptible to pitting corrosion in aqueous bromide solutions under potentiodynamic technique. The oxide film stability was affected by the nature of the electrolyte, scanning rate and applied potential. Also, a steady state Ti/ TiO_2 electrolyte system was observed. The oxide film thickness and the formation rate reached their highest values in $MgBr_2$ solutions.

Introduction

Titanium and titanium passive films have often been taken as a standard case in investigations concerning corrosion, passivation, electrochemical and photo-electrochemical behavior of valve metals [(1)]. Most investigations have been carried out in acid media, e.g. H_2SO_4 [(2-8)], HNO_3 [(9,10)] and H_3PO_4 [(11)]. Additionally, the influence of hydrofluoric acid and fluoride ion on the corrosion and passive behavior of titanium was studied [(12-14)]. Anodic and cathodic Tafel slopes at different current densities were calculated in aqueous chloride solutions [(15-18)]. Recent investigations have shown the behavior of pure titanium in organic acids [(19)] and sea water [(20)].

Titanium and some of its alloys are used in large scale for dental applications due to their excellent corrosion resistance and mechanical properties [(21,22)]. The electrochemical behavior in artificial saliva containing H_2O_2 was studied using open circuit potential, polarization and electrochemical impedance spectroscopic techniques [(23)].

The present work is a systematic study of the stability of the oxide films in different bromide solutions and the factors affecting such stability.

Experiment

The electrochemical cell was a three- electrode cell (capacity 50 ml). The working electrode was made of massive cylindrical, spectroscopically pure titanium rod (Aldrich - Chemie). A stout copper wire was employed as electrical contact. The

electrode was fitted into glass tubing of appropriate internal diameter with epoxy resin, leaving a cylindrical surface area of 2.23 cm^2 to contact the electrolyte. A platinum sheet was used as counter electrode. The potentials were measured against a saturated calomel electrode with the aid of digital multimeter (KEITHLEY, model 175, USA). Potentiodynamic polarization measurements were generated using a Wenking Electronic Potentioscan model 73.

All measurements were carried out at room temperature. The electrolytic solutions were prepared using analytical grade reagents and bidistilled water.

Before each experiment the electrode surface was mechanically polished using successive grades of emery paper followed by washing with bidistilled water. In this way, the electrode surface acquired reproducibly silvery bright surface. The electrode was rinsed with bidistilled water and quickly transferred to the test solution where the measurements were carried out immediately.

Results And Discussion

Open circuit potential measurements

The potential of the titanium electrode was traced over a period of 120 minutes in naturally aerated aqueous solutions of hydrobromic acid, sodium bromide and magnesium bromide as illustrated in Figures (1, 2 and 3), respectively. These media covered concentration range from 0.05 to 1 M solution. In all solutions, the electrode potential got more positive with time indicating the tendency of Ti for passivation. The shift of electrode potential towards nobel values signified the repair and further thickening of the air- formed, pre-immersion oxide film on the surface of the metal [(24)].

In HBr solutions, there were positive shifts in potential till steady state values (Figure 1). The magnitudes of these positive shifts were increased with increasing concentrations. The same behavior was observed in $MgBr_2$ solutions but with no indication of a constant steady potential value (Figure 3). In NaBr solutions, there were positive shifts in potential with time as in $MgBr_2$ solutions but the potential was decreased to more active values with increasing concentrations. Also, in 0.3, 0.2 and 0.1M NaBr solutions, the potential values coincide with each other with increasing time. All curves were characterized by an instantaneous rise of potential which occurred within 1- 2 minute followed by an intermediate increase within which the potential rises gradually and linearly with time.

The results revealed that E_{imm} and E_{ss} were concentration dependent over the studied whole concentration range (Figure 4 and 5).

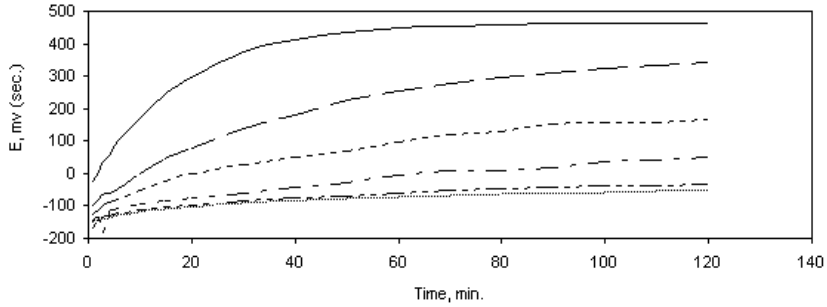

Figure (1): Potential- time curves of Ti in different concentrations of HBr

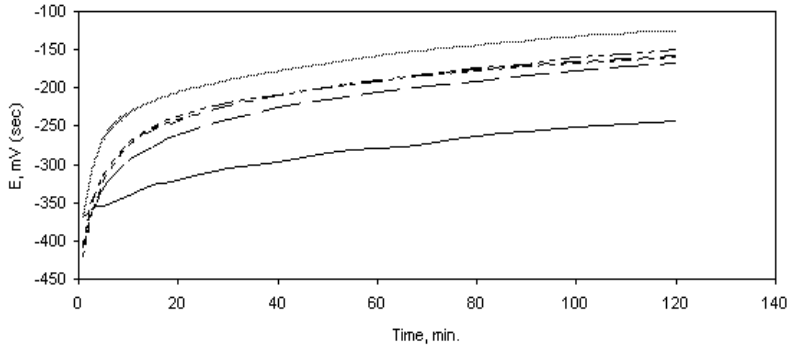

Figure(2): Potential- time curves of Ti in different concentrations of NaBr

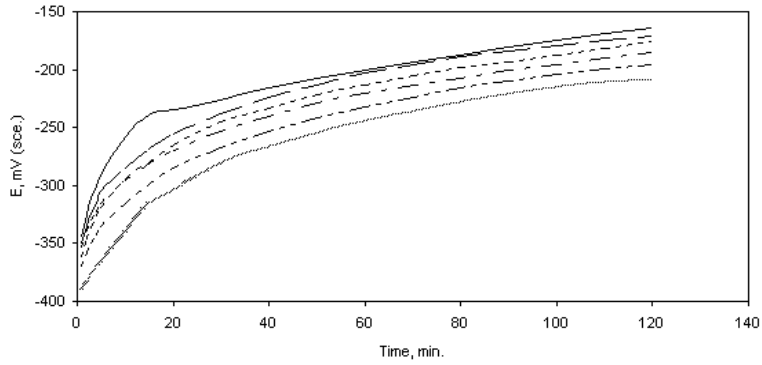

Figure (3): Potential- time curves of Ti in different concentrations of $MgBr_2$

1 M — 0.5 M - - - - - 0.3 M - - — 0.2 M - - - — 0.1 M ····· 0.05 M

The linear relation of these figures can be represented mathematically as:

$E = a + b \log c$ ---------- (1a)

Where:

E, is the immersion or steady state potential value.

a, is constant depending on the nature of solution.

b, is the slope of the linear relation.

Equation (1a) could be applied for E_{imm} and E_{ss} for each of the three solutions except for E_{ss} for NaBr solution where the equation became:

$E = a - b \log c$ ---------- (1b)

The passivity of Ti electrode in the solutions studied was increased in the following order: NaBr < $MgBr_2$ < HBr (Figure 4).

The slope b values of the linear relations were 426.8, -74.7 and 222.6 mV/ log c for HBr, NaBr and $MgBr_2$, respectively (Figure 5). The high slope positive value of HBr indicated the high concentration effect of the solution in the direction of increasing concentration. In concentrations less than 0.05M HBr (0.0378, 0.01 and 0.001M) the E_{ss} was independent of concentration.

For a reaction [25]:

M | M+ (aq, L)|| M+(aq, R) | M

The familiar Nernest equation is:

$E = E° - 0.059/ n \ln Q$, $Q = a_L/a_R$ ---------- (2)

Equation 2 and values of slope b of Figure 5 were used to calculate the number of electrons transferred in each test solution which was nearly 2 electrons for NaBr and $MgBr_2$ solutions whereas equaled to 0.11 electron for HBr solution. For Ti metal the electrode reactions were [26,27] :

$Ti^{+} + \bar{e} = Ti(s)$ $E° = 0.3363$ V ---------- (3)

$Ti^{+2} + 2\bar{e} = Ti$ $E° = -1.63$ V ---------- (4)

$Ti^{+3} + \bar{e} = Ti^{+2}$ $E° = -0.37$ V ---------- (5)

$Ti^{+4} + \bar{e} = Ti^{+3}$ $E° = 0.00$ V ---------- (6)

From all these reactions, equation 4 coincided with this work.

The changes of electrode potential towards positive values were accompanied by corresponding equivalent increase in thickness of the oxide film. The equation, which described the variation of the electrode potential with time for metals carrying thin oxide films, could be represented by:

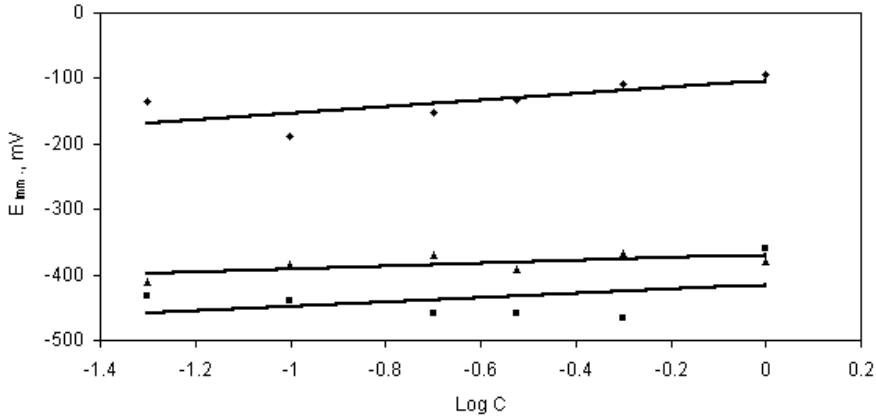

Figure (4): E $_{mm.}$ vs log C for Ti in different Br^- solutions

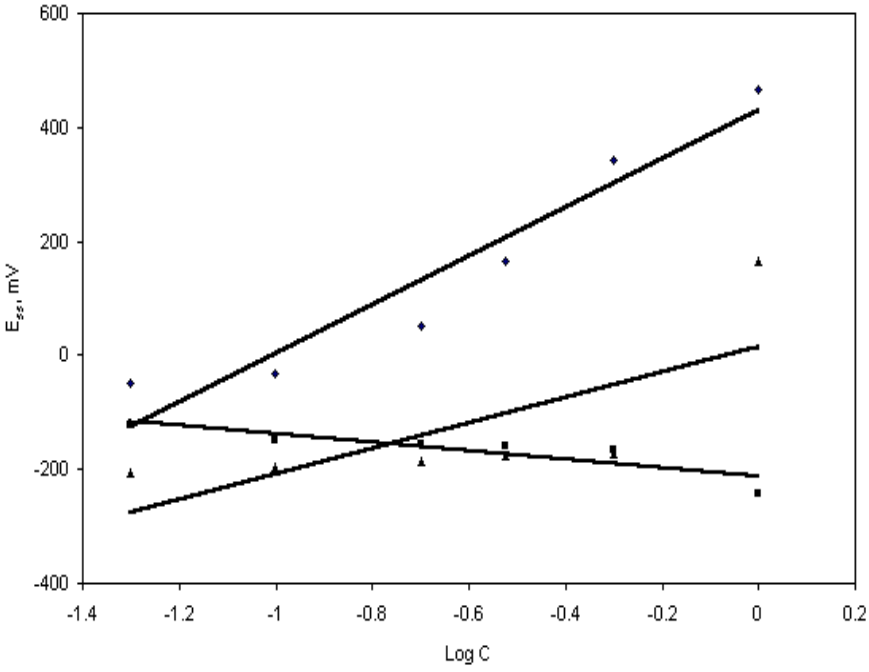

Figure (5): E_{ss} vs log C for Ti in different Br^- solutions

♦ HBr ■ NaBr ▲ MgBr2

$$|E| = \text{Cons.} + 2.303\,(\delta/\beta)\log t \quad \text{----------} \quad (7)$$

Where:

δ, is the rate of oxide thickening per unit decade of time. The term β is identified as [28]:

$$\beta = n\,F/\,RT\,\alpha\,\delta^{-} \quad \text{----------} \quad (8)$$

Where,

α, is the charge transference coefficint encountered in normal electrochemical processes ($0 < \alpha < 1$)

δ^{-}, is the height of the energy barrier surmounted during charge transfer.

The value of α was taken as 0.5 while δ^{-} was 1 nm and n= 2 electrons for NaBr and $MgBr_2$ solutions. Accordingly, β aquired the value of 39 nm/ V for NaBr and $MgBr_2$ solutions while for HBr, β was 2.14 nm/ V. The slopes of the E vs. log t plots and the computed values of film thickness δ, for the Ti electrode in all solutions are listed in Table (1).

Table (1): Values of immersion potentials ($E_{imm.}$), and steady state potentials ($E_{ss.}$), slopes (b), and rates of oxide film thickening of Ti electrode in different Br^{-} solutions at different concentrations

Conc. (M)	Test solution	$E_{imm.}$ (mV)	$E_{ss.}$ (mV)	b (mV/log t)	Rates of oxide film thickening (nm/log t)
1	HBr	-95	465	250.0	0.232
0.5		-109	344	64.10	0.059
0.3		-134	166	53.57	0.049
0.2		-153	50	60.60	0.056
0.1		-189	-33	47.62	0.044
0.05		-135	-50	25.00	0.023
1	NaBr	-361	-243	36.36	0.615
0.5		-465	-167	116.6	1.975
0.3		-460	-159	155.8	2.639
0.2		-460	-157	155.5	2.634
0.1		-439	-150	128.5	2.177
0.05		-433	-124	161.9	2.742
1	$MgBr_2$	-379	-164	85.00	1.439
0.5		-368	-171	3.340	0.056
0.3		-391	-176	73.33	1.241
0.2		-369	-185	65.22	1.104
0.1		-383	-196	60.87	1.031
0.05		-410	-207	43.75	0.740

The rates of oxide film thickening in HBr and $MgBr_2$ solutions were found to increase with increasing the test solution concentration (Table 1). On the other hand, the slopes in case of NaBr solutions were found to be independent of concentration. This stage (the first 10 minutes), which directly preceded the attainment of the steady state potential apparently represented the formation of films actually responsible for the high corrosion resistance of the metal.

Potentiodynamic Measurements

Effect of corrosive medium

The potentiodynamic anodic and cathodic polarization curves of Ti in three different 0.001M Br^{-} solutions at a constant scanning rate of 1 mV/ sec was

represented in Figure (6). The general aspects that drawn from this figure could be described as follows: when the electrode potential was made to change towards positive values, the initially high cathodic current density decreased continually and changed its direction at a definite potential (zero - current potential E°), at which the rate of cathodic reaction was equal to the rate of anodic one. The cathodic current was due to the overall reaction:

$2H^+ + 2\bar{e} = H_2$ ---------- (9)

However for the far removal of the potential from E°, illustrates the observed active dissolution region where the potential- current relations were linear with the well-defined Tafel slope. A passive potential region began approximately at +50 to +200 mV (sce) for all solutions. Finally, transpassive region and oxygen evolution took place by the reaction:

$2H_2O = O_2 + 4H^+ + 4\bar{e}$ ---------- (10)

Depending on the nature of the metal/solution system, the passive region might be associated with gas evolution or corrosion of the metal. In this study both processes proceed simultaneously.

The values of E_{corr} and I_{corr} were determined from the extrapolation of cathodic and anodic Tafel lines intersected at the zero- current potential and tabulated in Table (2).

Ti in the three different Br^- solutions showed the same behavior. The passivation rate (P_R) was increased in the following order $MgBr_2$< NaBr< HBr. This could be attributed to the smaller size of hydrogen atom as compared with that of Na atom and Mg atom of the largest size. This ensured faster mobilities and greater coverage of the metallic surface. The obtained results indicated that the passivation rate depended on the nature of the electrolyte.

Table (2): Comparison of electrochemical parameters in the three different Br^- solutions

Test solution	HBr	NaBr	$MgBr_2$
E_{corr}, mV(sce)	-32	-65	-74
I_{corr}, μA/cm^2	2.6	2.9	4.5
I_p, μA/cm^2	30	35	40
E_{pp}, mV(sce)	80	90	90
E_{ps}, mV(sce)	220	230	200
B_a, mV/decade	1667	5106	2400
B_c, mV/ decade	1667	1905	2000
P_R, mmpy	259	228	147

$E_{corr.}$, corrosion potential $I_{corr.}$, corrosion current $I_{p.}$, passivation current
$E_{pp.}$, primary passivation potential $E_{ps.}$, secondary passivation potential
Ba., anodic Tafel slope Bc., cathodic Tafel slope $P_{R.}$, passivation rate.

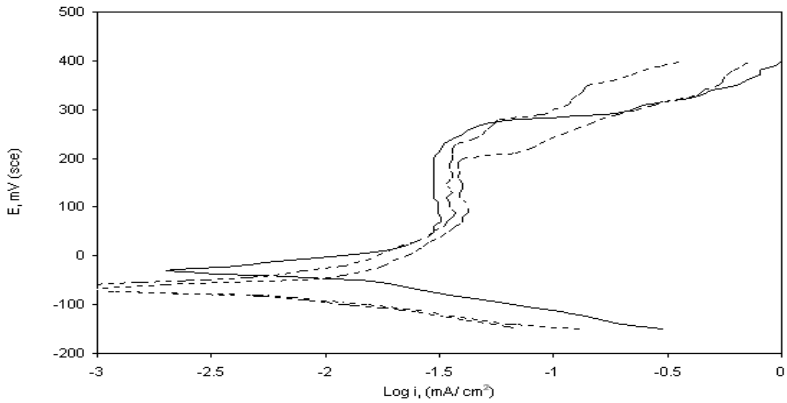

Figure (6): E- log i curves of Ti electrode (effect of corrosive medium)

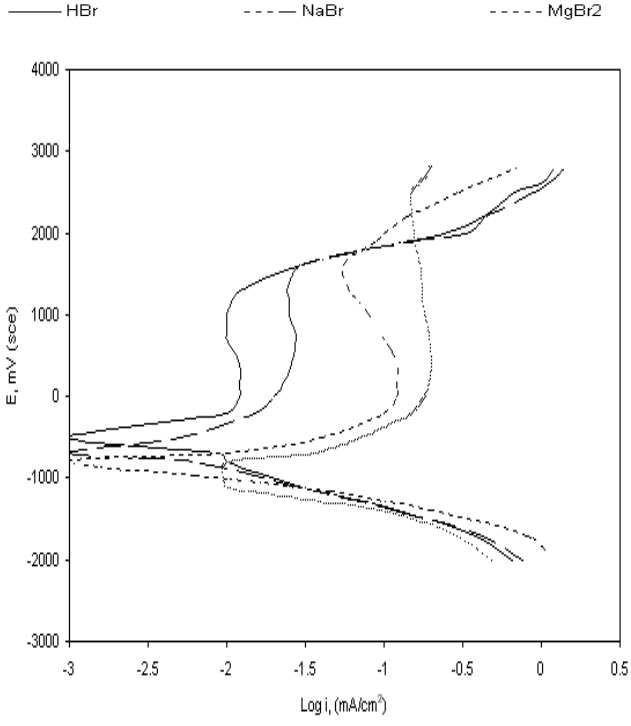

Figure (7): E- log i curves of Ti electrode in 0.001M $MgBr_2$ (effect of scannning rate).

Effect of scanning rate:

The current densities at different potentials of Ti traced in 0.001M $MgBr_2$ solution at different scanning rates of 2, 5, 10 and 20 mV/ sec could be plotted to produce polarization curve as given in Figure (7). Results revealed the following characteristics:

i. An active dissolution region was observed where the potential- current relations were linear with the well-defined Tafel slopes.

ii. A current curved region signifying the transition from active dissolution to passive state on the Ti surface was denoted.

iii. A transpassive potential region began, followed by oxygen evolution at which the current density increased sharply with little increase in potential.

It was found that active and passive regions were function of the scanning rates (Figure 7). The decrease of scanning rate was accompanied by decrease of the current density (I_p) required to produce passivity. The results showed that I_p equaled 10, 26, 120 and 200 μA/ cm^2 for 2, 5, 10 and 20 mV/sec, respectively. Thus, scanning rate decrease led to the attainment of the passive state, indicating that the time of anodization played an important role in the passivation process.

It is worthy to note that in studying the effect of both corrosive medium and scanning rate, the electrode surface after the time of experiment showed the presence of several large corrosion pits. This was achieved even at low concentration (0.001M) and at low scanning rate (1mV/sec). Such finding confirmed that, Ti might be susceptible to pitting corrosion in aqueous bromide solutions, which was in harmony with those obtained by previous investigator [29].

*Potentiostatic polarization***:**

At a constant potential of +200 mV, the rapid decrease in the current to values of few microamperes (30, 50 and 10 μA/ cm^2) for 0.001M HBr, NaBr, and $MgBr_2$ solutions respectively, was an indicative of passivation of the electrode (Figure 8). Previous work ensured that, the decrease of the anodic current coincided with the active dissolution of Ti metal to Ti^{3+} and also to the passivation of titanium [18]. This might be illustrated by the following proposal: Ti metal owed its corrosion resistance in certain media to the formation of massive bulk protective film on its surface. These films differ from the usual passivating films in that they are readily visible and much less tenacious [30].

The rise of the anodic current with increasing time at applied potential of -100 mV, was clear in HBr solution and was actually an indicative of oxide film rupture.

This could occur by forming a metal bromide at the metal oxide interface, (Figure 9). This corresponded to the oxidation of Br^- at the TiO_2 surface as reported previously [29]. For NaBr and $MgBr_2$ solutions, the rise of the anodic current was very little indicating the relative high stability of the oxide formed in these solutions.

For a constant applied voltage, the potential at the oxide/ solution interface would be less positive for a thicker film, resulting in a decrease in the concentration, or chemisorption of Br^- at the interface [31]. The breakdown of the film, as indicated by the abrupt increase in the current density, could be anticipated based on this mechanism as a result of the rapid increase in the interfacial potential as the film became thinner [29].

Generally the current density was increased as the applied potential increased (Figure 10). At applied potential of -300 mV, a sharp increase in currents was observed from -1500 to -900 $\mu A/cm^2$ within 20 sec. The decrease in the passive film stability indicated by increasing c.d. might be due to the increasing number of defects in the oxide film matrix[32]. At -200, -100, and 0.0 mV; the current showed no changes with time and remains constant. This could be due to the high stability of the oxide films at these potentials reflecting the formation of a highly ordered and less defective oxide films. At +100 and +200 mV, the current dropped more sharply attaining a constant value of few microamperes (50 $\mu A / cm^2$). The drop of currents declared the formation of a new passive layer. At +300 mV, the current dropped at the first 10 seconds then increased smoothly till reaching steady state at 760 $\mu A / cm^2$ within 20 sec. It could be assumed that the increase in current density was due to the dissolution of the passive layer formed. This could be explained by the dissolution of Ti via the formation of soluble bromo- complexes. Studying the effect of Cl^- ions on the same metal showed the same behavior [17]. This meant that the stability of the oxide film was affected by the applied potential.

It was speculated that chemisorption of Br^- would be most pronounced at positive potentials promoting the formation of Ti - Br bonds at the oxide/ solution interface and subsequently oxide dissolution [29].

Applied potential values more positive than zero caused the passivation of the surface towards Br^- oxidation. On the other hand, for potential values less than zero the observed increase in the thickness of oxide layer was responsible for the observed decrease in the rate of Br^- oxidation [29]. Although the rate of Br^- oxidation was sufficiently large, the smaller currents indicated that the reaction proceeded at a kinetically controlled rate.

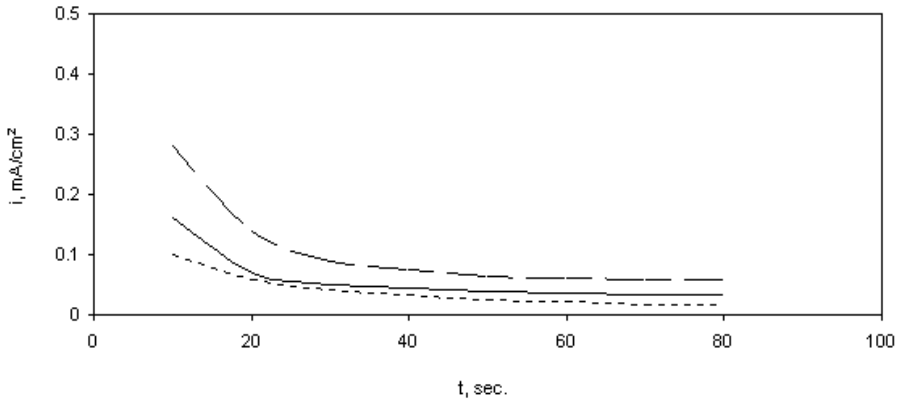

Figure (8): Potentiostatic polarization curves for Ti in 0.001Mf different Br^- solutions at +200 mV

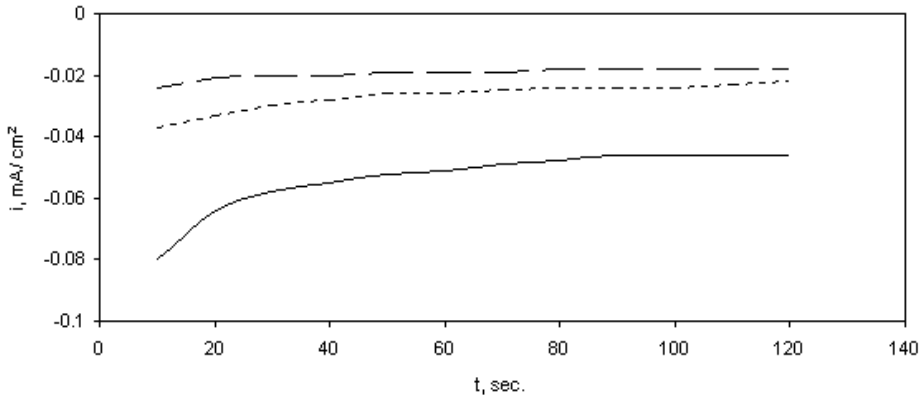

Figure (9): Potentiostatic polarization curves for Ti in 0.001 M different Br^- solutions at -100 mV

——— HBr — — NaBr - - - - - MgBr2

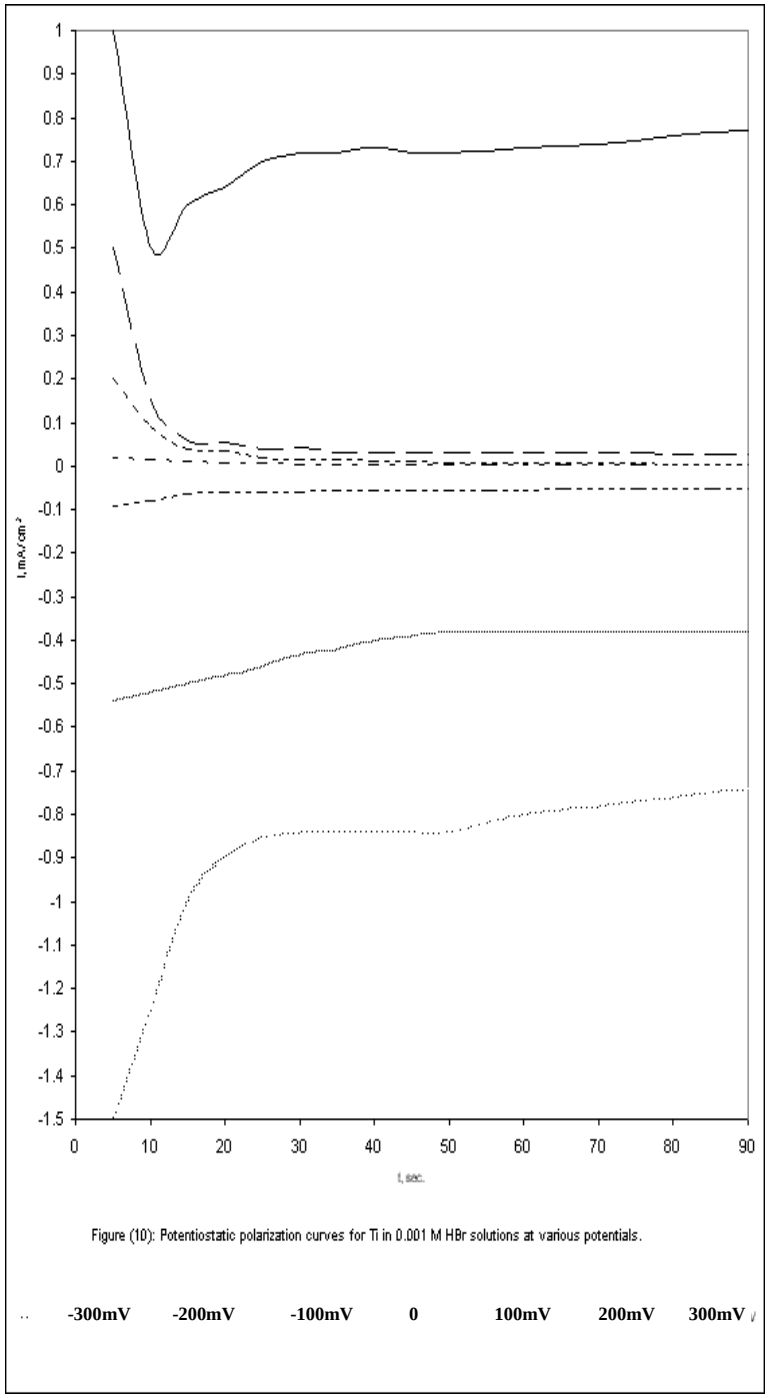

Figure (10): Potentiostatic polarization curves for Ti in 0.001 M HBr solutions at various potentials.

Galvanostatic polarization:

Galvanostatic measurements carried out in 0.001M Br^- solutions at various constant current densities ranging from 10 to 100 $\mu A/cm^2$ are illustrated in Figures (11,12 and 13).

Passivation in all applied current density ranges for all solutions was observed. The shape of the curves was characterized by presence of a peak potential before stabilization potential. Thus firstly, the potential increased passing through a maximum value. Then, it decreased gradually within a few minutes till reaching steady state potential with increasing time. It was suggested that in bromide solutions, an oxide of Ti (particularly the dioxide) was sufficiently stable since a steady state Ti/TiO_2 electrolyte system was established. For all solutions during the first several seconds, which were not included in the diagram, the initial rise of potential was attributed to the removal of hydrogen ions adsorbed to the electrode surface as well as to the charging of the anodic double layer [18]. This process would continue with the potential rise gradually and linearly with time, which was believed to be due to the oxide film formation and thickening. The rate of oxide film perfection was limited when reaching the primary passivation potential (E_p) i.e. the potential associated with the peak. The process, after which this peak was attained, was the redistribution of the interface potential difference. After this point, the thickness of the TiO_2 film showed no longer significant increase. Eventually, the film began to break down, and dissolution of Ti via complex formation occurred[17].

The equation representing the chemical dissolution of the oxide film is [18]:

$TiO_2 + 2H^+ = TiO^{2+} + H_2O$ ---------- (11)

While that representing the electrochemical dissolution of the metal through the oxide film is:

$Ti + H_2O = TiO_2^{2+} + 2H^+ + 4\,\bar{e}$ $\quad E° = -0.88V$ ---------- (12)

The stabilized potential limit was believed to be caused by a state of equilibrium where the rate of film thickening was equal to the rate of dissolution. A linear relation was observed between the stabilized potential and increasing current density as a result of an increase of the passive film layer.

In all solutions, the increase in current density caused an increase in E_{ss}. and E_p, which could be due to the passivation of Ti electrode in the test solutions. The surface charging capacity C_s reached its maximum value in HBr at 10 and 100 $\mu A/cm^2$, while in NaBr and $MgBr_2$ solutions reached their maximum values at 75 $\mu A/cm^2$. The results also showed that the amount of electricity involved in the

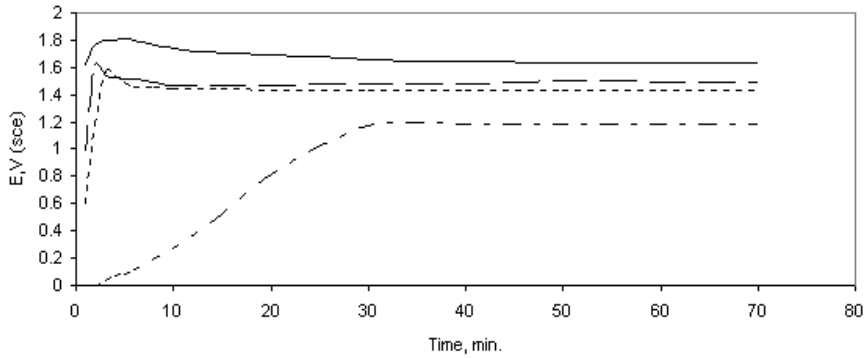

Figure(11): Galvanostatic polarization curves for Ti in 0.001M HBr at different current densities

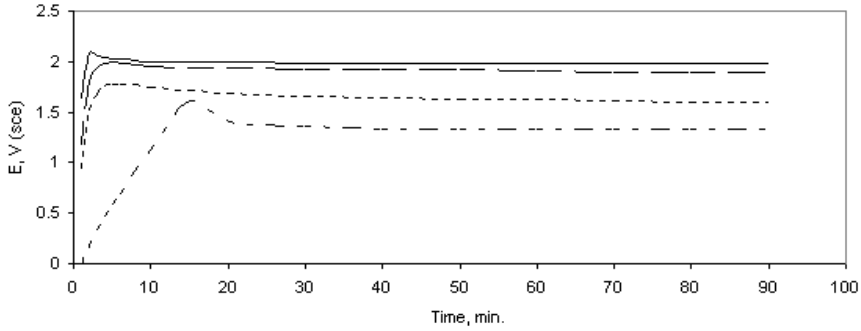

Figure (12):Galvanostatic polarization curves for Ti in 0.001M NaBr at different current densities

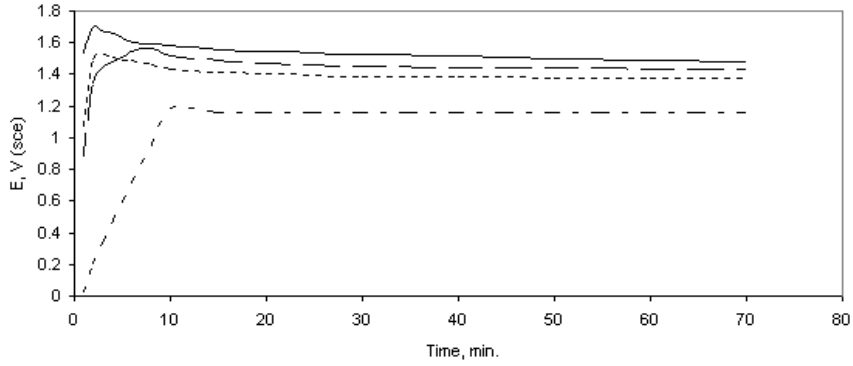

Figure (13): Galvanostatic polarization curves for Ti in 0.001M $MgBr_2$ at different current densities

10 µA/cm2 50 µA/cm2 75 µA/cm2 100 µA/cm2

formation of the oxide (Q) increased with an increase in the current density for NaBr solutions. The high Q values were due to the preferential adsorption of Br^- ions on the oxide surface acting as a depolarizer for the main anodic process of oxygen discharge[17]. In HBr and $MgBr_2$ solutions, the values of Q did not change regularly with the polarizing current density (Table 3).

Anodic polarization at constant current density led to film growth which might occur by the transport of positive ions through oxide to the oxide/ solution interface or by transport of oxide ions in the opposite direction. This was achieved through the following equation[1]:

$$\Delta\delta = (M/ S\sigma nF)\,\Delta Q \quad \text{----------(13)}$$

Where:

M, is the molecular weight of oxide = 79.9 g/ mol

S, its density = 3.9 g/ cm^3

σ, is the roughness factor = 3

n, is the number of Faradays F required for the formation of one mole oxide[17].

Table (3): Electrochemical polarization data of Ti in different Br^- solutions at different current densities

Test solution, 0.001M	C.d. ($\mu A/cm^2$)	E_{ss} (V)	E_p (V)	τ_p (sec)	Q X 10^4 ($\mu C/cm^2$)	C_s ($\mu F/cm^2$)	$1/C_s$ ($\mu F^{-}cm^2$)
HBr		1.180	1.172	1800	1.8	15.35	0.065
NaBr	10	1.337	1.607	900	0.9	5.600	0.178
$MgBr_2$		1.160	1.188	600	0.6	5.050	0.198
HBr		1.435	1.570	180	0.9	5.732	0.174
NaBr	50	1.593	1.777	300	1.5	8.441	0.118
$MgBr_2$		1.380	1.540	60	0.3	1.948	0.513
HBr		1.495	1.616	120	0.9	5.569	0.179
NaBr	75	1.900	1.990	300	2.25	11.31	0.088
$MgBr_2$		1.435	1.560	480	3.60	23.08	0.043
HBr		1.638	1.810	300	3.00	16.57	0.060
NaBr	100	1.995	2.080	120	1.20	5.769	0.173
$MgBr_2$		1.475	1.700	120	1.20	7.058	0.142

$E_{ss.}$, steady state potential $E_{p.}$, primary passivation potential

$1/C_s$, reciprocal capacity Q., amount of electricity involved in the formation of the oxide

C_s, the surface charge capacity $\tau_{p.}$, the maximum passivation time

In fact, the total oxide thickness was composed of δ°, (thickness of the initial oxide present after the polishung step) and ΣΔd (oxide resulted from the successive anodizing steps) as reported by Kerrec on his work on Ta, which led to the equation [33]:

$$\delta = \delta^\circ + \Sigma\Delta d \quad \text{Or} \quad \delta = \delta^\circ + vit/\sigma \text{ ----------(14)}$$

Equation 14 was derived from equation 13 by replacing (M/SnF) by the volume of oxide formed per coulomb, which is denoted by v. From calculations of film thickness, it was observed that, the film reached its maximum thickness in HBr solution at 100 $\mu A/cm^2$ which equaled to 0.531 A°. In NaBr and $MgBr_2$ solutions, the film reached its maximum thickness at 75 $\mu A/cm^2$ which equaled to 0.398 and 0.637 A°, respectively.

Pilling and Bedworth[34] proposed that oxidation resistance should be related to the volume ratio of oxide and metal. Mathematically, this could be expressed as:

$$R = Wd/Dw \text{ ----------} \quad (15)$$

Where:

W, is the molecular weight of the oxide.
w, is the atomic weight of the metal.
D, is the specific density of the oxide.
d, is the specific density of the metal.

The ratio R indicates the volume of oxide formed from a unit volume of metal. It was argued that a ratio much greater than 1 (R= 1.95 for Ti) tended to introduce large compressive stresses in the oxide which caused poor oxidation resistance due to cracking and spalling [34].

Formation rates $(dE/dt)_i$ were calculated from the expanded E/ t relations at the first 180 sec. (Table 4).

HBr solution had the smallest formation rate at the smallest current density. The highest formation rate was observed in $MgBr_2$ solution at the highest c.d. value. This might be due to the small size of hydrogen atom and the large size of Mg atom.

Table (4): Comparison of formation rates in the three different Br^- solutions

C.d. ($\mu A/cm^2$)	Formation rates $(dE/dt)_i$		
	HBr	NaBr	$MgBr_2$
10	0.59	2.55	2.22
50	8.33	8.33	16.66
75	10	11.25	17.66
100	12	14.58	20

The application of anodic current to a structure should lead to increase the dissolution rate of a metal and decrease the rate of hydrogen evolution. This usually occurred except for metals with active passive transitions such as Ti as illustrated in potentiodynamic measurements[35]. If carefully controlled anodic currents are applied to these metals, they are passivated and the rate of metal dissolution is decreased [35]. Subsequently the formation rates of oxide thickening increased with increasing current density (Table 4).

Conclusion

It could be concluded that open circuit potential measurements indicated the tendency of Ti for passivation in the studied three different bromide solutions. Titanium was susceptible to pitting corrosion in aqueous bromide solutions under potentiodynamic conditions. The stability of the oxide film formed was affected by the nature of the electrolyte, scanning rate and applied potential. Under galvanostatic conditions, a steady state Ti/TiO_2 electrolyte system was established. The oxide film thickness and the formation rate reached their highest values in $MgBr_2$ solution due to the large size of Mg atom.

Acknowledgment

The author would like to express her deep gratitude and sincere appreciation to Professor Dr. Amal S. I. Ahmed, Professor of Electrochemistry, Department of Chemistry, Faculty of Science (Girls), Al- Azhar University, for her valuable assistance during the experimental work and providing the working metal.

References

1. A. AMMAR and I. KAMAL; Electrochim. Acta, 16 pp. 1539 (1971).
2. W. A. BADAWY, S. S. Elegamy and Kh. M. Ismail; J. Br. Corros., 28 (2) pp. 133 (1993).
3. E. MC- CAFFERTY; Corros. Sci., 47 (12) pp. 3202 (2005).
4. W. B. UYOMO AND S. W. DONNE; Electrochim. Acta, 51 (16) pp. 3338 (2006).
5. ISMAEEL N. Andijani, Shahreer Ahmad and Anees U. Malik; Desalination 129 (1) pp. 45 (2000).
6. J. KRÝSA, R. MRĀZ AND I. ROUŠAR; Materials Chemistry and Physics, 48 (1) pp. 64 (1997).
7. ZHIYU JIANG, JIANGTAO WANG, QIAN HU AND SIYA HUANG; Corros. Sci., 37 (8) pp. 1245 (1995).

8. S. M. A. HOSSEINI AND V. B. SINGH; Materials Chemistry and Physics, 33 (1-2) pp. 63 (1993).

9. M. MASMOUI, D. CAPEK, R. AABDELHEDI, EL HALOUANI AND M. WERY; Surface and Coatings Technology, 200 (24) pp. 6651 (2006).

10. W. A. BADAWY AND F. M. AL-KHARAFI; Bulletin of Electrochemistry 12 (9) pp. 505 (1996).

11. V. B. SINGH AND S. M. A. HOSSEINI; Corros. Sci., 34 (10) pp. 1723 (1993).

12. GERT BOERE; J. Applied Biomaterials 6 (4) pp. 283 (1995).

13. KEN'ICHI YOKOYAMA, Toshio Ogawa, Kenzo Asaoka and Jun'ichi Sakai; Materials Science and Engineering A, 384 (1- 2) pp. 19 (2004).

14. SHINJI TAKEMOTO, Masayuki Hattori, Masao Yoshinari, Eiji Kawada and Yutaka Oda; Biomaterials 26 (8) pp. 829 (2005).

15. D. G. KOLMAN AND J. R. SCULLY; J. Electrochem. Soc., 143 (6) pp. 1847 (1996).

16. G. T. BURSTEIN AND R. M. SOUTO; Electrochim. Acta, 40 (12) pp. 1881 (1995).

17. S. I. AHMED, K. J. FRIESEN AND A. S. ABD- EL- AZIZ; Intl. J. of Science and Technology 12 (1) pp. 5 (2000).

18. S. I. AHMED, K. J. FRIESEN AND A. S. ABD- EL- AZIZ; Intl. J. of Science and Technology 12(1) p. 17 (2000).

19. MARIE KOIKE AND HIROYUKI FUJII; Biomaterials 22 (21) pp. 2931 (2001).

20. Kalid S. E. Al- Malahy and T. Hodgkiess; Desalination, 158 (1- 3) pp. 35 (2003).

21. G. MABILLEAU, S. BOURDON, M. L. JOLY- GUILLOU, R. FILMON, M. F. BASLÉ AND D. CHAPPARD; Acta Biomaterialia, 2 (1) pp. 121 (2006).

22. J. PAN, D. THIERRY AND C. LEYGRAF; Electrochim. Acta, 41 (7- 8) pp. 1143 (1996).

23. N. A. AL- MOBARAK, A. M. AL- MAYOUF AND A. A. AL-SWAYIH; Materials Chemistry and Physics, 99 (2- 3) pp. 333 (2006).

24. U. R. EVANS; The Corrosion and Oxidation of Metals, pp. 898 2nd ed. Arnold, London (1961).

25. P. W. ATKINS; Physical Chemistry Atkins, pp. 260 6th ed. Oxford (1998).

26. Samuel H. Maron and Carl F. Prutton; Principles of Physical Chemistry, pp. 488 4th edition (1972).

27. P. W. ATKINS; Physical Chemistry Atkins, pp. 937 6th ed. Oxford (1998).

28. K.J.VETTER AND W. WIEDERHOLT; Passivierende Film and Deckschichten 72, (1956), (Berlin, Springer Verlag)

29. H. S. WHITE; J. Electrochem. Soc., 141 (3) pp. 636 (1994).

30. MARS G. FONTANA AND NORBERT D. GREENE; Corrosion Engineering (Chapter 2) pp. 20 2nd ed. (1978).

31. P. Smith and H. S. White; Anal. Chem., 64 pp. 2389 (1992).

32. W. A. BADAWY AND KH. M. ISMAIL; Electrochim. Acta, 38 (15) pp. 2231 (1993).

33. O. Kerrec; D. Devilliers ; H. Groult ; M. Chemla; J. Electrochim. Acta 40 (6), 719- 24 (1995).

34. MARS G. FONTANA AND NORBERT D. GREENE; Corrosion Engineering (Chapter 11) pp. 347, 2nd ed. (1978).

35. MARS G. FONTANA AND NORBERT D. GREENE; Corrosion Engineering (Chapter 6) pp. 211, 2nd ed. (1978).